JOURNAL OF SPACECRAFT AND ROCKETS
Vol. 48, No. 2, March–April 2011

Progress on the Physical Approach to Molecular Contamination Modeling

J-F. Roussel,* T. Tondu,† and T. Paulmier‡
ONERA, 31055 Toulouse, France
D. Faye§
Centre National d'Etudes Spatiales, 31401 Toulouse, France
and
M. Van Eesbeek¶ and R. Rampini**
ESA, 2200 AG Noordwijk ZH, The Netherlands

DOI: 10.2514/1.49490

A review of the contamination physics and of the most widespread engineering approaches to contamination assessment was carried out. The two main approaches are the physical and the empirical one. The main questions still open to validate the physical approach to outgassing and deposit physics were then studied. Among others, special attention was paid to the important point of a realistic separation of chemical species, probably a prerequisite for a physical modeling. Several original results were obtained. Some lead to a quite clear conclusion, like the preeminence of the limitation by desorption over the limitation by diffusion for outgassing. This observed trend needs yet to be validated on other materials. Other major results are progress on the validation of the physical approach and on the ambitious species separation program.

Nomenclature

D	=	Fick's law diffusion coefficient, $cm^2.s^{-1}$
E_A	=	activation energy, $J.K.mol^{-1}$
f	=	contaminant flux density, $g.cm^{-2}.s^{-1}$
k	=	outgassing kinetic constant, s^{-1}
L	=	effective diffusion length of the sample, m
M	=	contaminant molar mass, g/mol
m, m_{evap}	=	deposited, evaporated or outgassed surfacic mass, $g.cm^{-2}$
m_0	=	contaminant monolayer mass, $g.cm^{-2}$
n_{vol}	=	contaminant volume density, $g.cm^{-3}$
n_{surf}	=	contaminant surface density, $g.cm^{-2}$
P_S	=	saturation vapor pressure, mbar
R	=	gas constant, 8.314 $J.K.mol^{-1}$
T	=	temperature, K
t	=	time, s
W	=	relative contaminant mass, %
τ	=	outgassing or deposit evaporation characteristic time, s

I. Introduction

IN THE last ten years many contamination studies were performed in collaboration between CNES (French space agency), ESA (European Space Agency), and ONERA (the French aerospace laboratory). A first important topic was the improvement of the physical approach to contamination, which has long been used in these institutes, since 1985 at ESTEC [1]. This is the subject of this paper. The synergy of photon-contamination interaction can result in significant surface property changes [2,3], however, this topic will not be treated in this paper.

The physical approach to contamination consists in modeling the phenomena of outgassing, deposition and reemission through mathematical laws aiming at the best possible approximation of the physical phenomena. It is in principle very powerful because it can address all situations in flight, as, e.g., thermal cycling and variable temperatures, inducing reemission. The involved physical phenomena are, however, complex, and a detail modeling of all of them is clearly impossible. Keeping present in mind that the final objective is contamination engineering and not science *per se*, the main guideline in this quest of a physical understanding of contamination processes must be to assess the relative importance of phenomena in the typical situations of interest, in term of materials, temperatures, etc. Then, the simplified physical view and simplified physical model that will be developed might prove useful for the engineer.

The contamination engineer needs to assess contamination deposits and their effects on various subsystems or functional materials. Very importantly, the contamination engineer must asses that at mission time scale for realistic conditions, e.g., with thermal cycling. The capability to extrapolate data obtained on ground during short experiments over years in flight is thus of the first importance.

This capability of extrapolating at very long times is a priori an important asset of a physical model, if successful. The alternative approach, consisting in a direct empirical extrapolation, must yet be considered carefully. If the more complex physical approach does not supply better extrapolations, it can somewhat be considered a failure. This is another motivation to improve and validate the physical approach.

This paper starts by reviewing contamination physics, needed to understand the next steps. The empirical and the physical approaches, as they are used today, are reviewed next. This is another prerequisite to a more detailed physical analysis. In the next section most questions still open in the physical approach are discussed. In a last section the focus is set on the major improvement idea, which would solve the weakest point of this approach, i.e., performing a realistic separation of the outgassed species. A good physical model can probably not be obtained before this new frontier is reached.

Received 20 February 2010; revision received 19 July 2010; accepted for publication 8 September 2010.

*Head of Space Environment Department; Jean-François.Roussel@onera.fr.
†Research Scientist, Space Environment Department; Thomas.Tondu@onera.fr.
‡Research Scientist, Space Environment Department; Thierry.Paulmier@onera.fr.
§Laboratory of Molecular Contamination: Delphine.Faye@cnes.fr.
¶Head of Materials Space Evaluation and Radiation Effects Section, TEC-QEM; Marc.van.Eesbeek@esa.int.
**Materials Space Evaluation and Radiation Effects Section, TEC-QEM; Riccardo.Rampini@esa.int.

II. Review of Physics

Contamination physics can be split in three steps, the emission of contaminants, their transport, and finally the physics of the deposit. The diversity of possible contaminant sources is large, including outgassing [1], thrusters [4], vents, dumps, material erosion [5] and so forth, but here focus shall be set on the frequently dominant source, outgassing.

A. Outgassing

Material outgassing itself can be seen as two successive steps: diffusion and desorption. Contaminant molecules embedded within the bulk material, such as, e.g., polymerization residues, additives, impurities, solvents, moisture, and so forth, must first diffuse to the surface (Fig. 1). Diffusion in polymers is a complex phenomenon and is not fully understood. Masaro and Zhu [6] present a review of the descriptions of this phenomenon. Diffusion can be Fickian, i.e., follow Fick's law, or non-Fickian [6]. The diffusion coefficient can strongly depend on contaminant concentration [7] and is significantly different below and above glass transition temperature. Furthermore contaminants can be dissolved or form clusters in the polymer. For all these reasons a really accurate diffusion description for all space materials is not realistic. For this reason it was assumed that diffusion can be described by Fick's law [Eq. (1)] with a temperature activated kinetic constant D:

$$f = D \cdot dn_{\text{vol}}/dx \tag{1}$$

Emission to vacuum is then conditioned by desorption. As discussed in [8], the desorption rate is linked to contaminant surface concentration by Henry law as long as no contaminant clusters exist in the polymer. The desorption flux f modeled by Eq. (2a) is then a first-order law with respect to the volume density at the surface n_{surf}. In Eq. (2b) the outgassing time τ follows an Arrhenius law

$$f = k(T) \cdot n_{\text{surf}} \tag{2a}$$

$$k = 1/\tau \tag{2b}$$

B. Transport

What is usually called transport includes line-of-sight transport, reflections on surfaces, and gas phase collisions. The physics involved in this field is globally known, although not necessary all cross sections or reflection distribution functions are, and it will not be further discussed here.

C. Deposit

The physics of the deposit shall be emphasized here. The condensation of impinging molecules is usually supposed to be total, although immediate bouncing is possible, in particular for supra thermal velocities. Evaporation of a pure contaminant thick layer follows the Langmuir law [Eq. (3)]. This emission law differs from the first-order law above describing desorption. A thick deposit rather follows an evaporation law with a flow rate independent of its thickness, i.e., an order 0 law, which can be related to its vapor pressure through Langmuir law for a pure contaminant. Mixing effects are discussed in Sec. IV

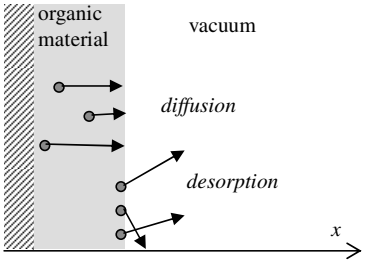

Fig. 1 Outgassing: diffusion followed by desorption.

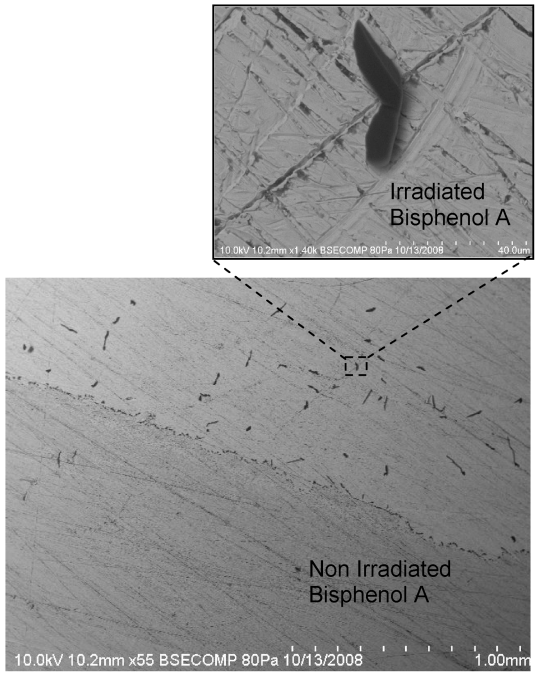

Fig. 2 Bisphenol A deposited as a film (lower part) or creating clusters (upper part).

$$\frac{\mathrm{d}m_{\text{evap}}}{\mathrm{d}t} = -0.044\sqrt{\frac{M}{T}}P_s(T) \tag{3}$$

A first complexity step stems from surface tension effects. Above some thickness, and depending of the molecule affinity with the substrate, thin films may tend to gather in clusters or droplets [9]. Figure 2 illustrates the evolution of a thin film to a cluster deposit. In this case clusters were observed after vacuum ultraviolet (VUV) irradiation of Bisphenol A. Details of the experimental setup can be found in [2]. Of course this may reduce the evaporation rates by orders of magnitudes. It is today extremely difficult to predict the formation of such clusters on different substrates, in particular in the case of a contaminant mixture and of possible extra interactions such as photochemistry. Mixing effects can also complicate this physics.

Chemistry is another huge source of complexity in the deposit, which is only briefly summarized here. UV photons can generate radicals or ions, initiating radical reactions finally leading to reticulation, photolysis, or chromophore creation [10]. Some recent advances in this field are reported in [2]. Another radical at the origin of such reaction is the ambient atomic oxygen. At first order it is usually considered as leading to the oxidization of silicones into silicates, hence a permanent deposit, and the erosion of other organic contaminant as confirmed by flight observations [11].

The detrimental effects of such deposits are essentially related to interactions with light. The most important is in most of the cases related to an increase of sunlight absorption by the generated chromophores or colored centers. It can impact thermal control, optical systems, solar cell power, etc. A change of infrared emissivity can also impact thermal control. Light diffusion can also become important, in particular in case of cluster formation.

III. Different Approaches to Contamination

The overall contamination processes described in previous section appears overwhelmingly complex. Space system engineers must yet produce contamination assessments as guidelines for design and for qualification. The experimental approach is usually limited to material testing. A refined assessment at system level is usually intractable experimentally and modeling is the preferred approach. The main difficulties are the complexity of the involved phenomena and the need to extrapolate necessarily short experiments to the year long space missions.

In this perspective several simplified approaches were developed. The first approach described is essentially empirical, while the second tries to model the most important physical phenomena through reasonably simplified laws.

A. Empirical Approach

The major attempt to address contamination assessment by a direct empirical approach is the ASTM 1559 standard [12]. Very briefly, this well known method consists in measuring on quartz crystal microbalances (QCMs) the deposition of contaminants originating from a sample material in an effusion cell (see Fig. 3). The temperatures of the outgassing material and of the QCMs are maintained constant over a few days. Different temperatures are tested for the emitter and the receiver. A thermogravimetric analysis (TGA) is usually performed at the end of the test to obtain information on the volatility of the condensed contaminants.

Based on these data, the practical assessment method for space missions is usually the following. Worst case temperatures are selected in the datasets with respect to flight data, i.e., the next warmer temperature for the source and the next colder for the deposition surface. The corresponding experimental data, extending over a few days, are then mathematically extrapolated to many year missions, through some power law or logarithmic law.

The pros of this method are its simplicity and directness. On the other hand it is limited, because, for example, no heating-based reemission can be modeled, and there is no real physical justification of the mathematical extrapolation to mission time scale.

As an illustration of the latter difficulty, four fits of a 96 h constant temperature collected volatile condensable mass (CVCM) were made by four different laws, two power laws and two logarithmic laws. They are displayed in Fig. 4. It is never possible to accurately fit such data by a single law over the whole period because the beginning is quite different. An accurate fit of the last two or three days was thus favored.

The next step was to extrapolate the fit to typical mission duration (see Fig. 5). Clearly the arbitrary choice of the fitting function can yield discrepancies close to a factor of 5 in this example. Logarithmic laws are more optimistic, while power laws are more conservative.

B. Physical Approach

More physical approaches managing the physical processes are also proposed for contamination assessment [13]. Since 1985 ESA developed such a physical approach [1]. The complex emission physics was simplified into a residence time approach, or 1st order law, representative of desorption, both for outgassing and reemission. Each characteristic time is supposed to follow an Arrhenius law [Eq. (4b)] usually linearized (in the exponential) to simplify computer treatment in the 1980s [Eq. (4c)]. The total contaminant mass, remaining in the outgassing material or deposited all over the spacecraft after transport computation, is then obtained as the sum of masses of all contaminant species α

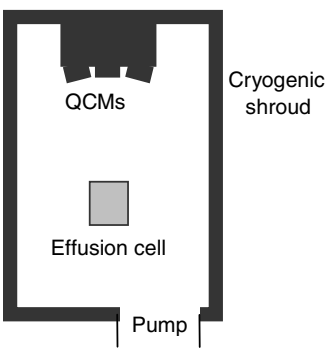

Fig. 3 A typical experimental setup for dynamical characterization of outgassing and condensation.

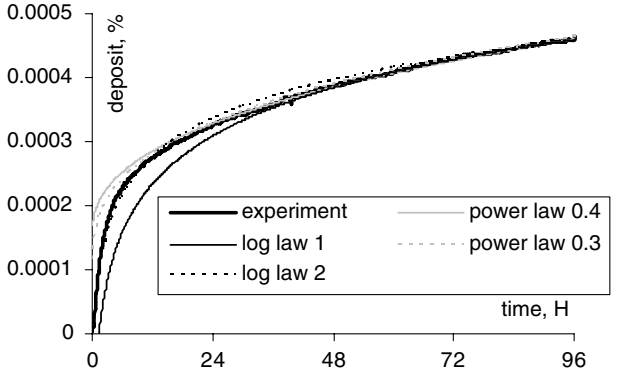

Fig. 4 Fit of an experimental EC2216 deposit at constant temperature (CNES data) by four different laws.

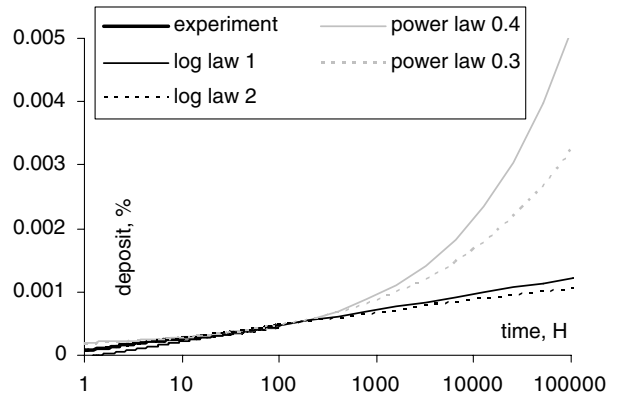

Fig. 5 Extrapolation of the four previous fits to mission time scale (100, 000 H = 11 years).

$$\frac{\mathrm{d}m^{\alpha}}{\mathrm{d}t} = -\frac{m^{\alpha}}{\tau^{\alpha}(T)} \tag{4a}$$

$$\tau^{\alpha}(T) = \tau_0^{\alpha} e^{E_A^{\alpha}/RT} \tag{4b}$$

$$\tau^{\alpha}(T) = \tau_0^{\alpha} e^{-k^{\alpha}(T-T_0)} \tag{4c}$$

This approach supplies temperature dependences. It allows thus physical extrapolation to any temperature profiles, and also to long term durations because a ground experiment at high temperature can be viewed as an accelerated experiment. Typical test procedures involve increasing temperature steps (Fig. 6). The acceleration at the steps allows extracting the temperature dependence factors of the Arrhenius-like laws for time constants (4b) or (4c). The experimental TML data are then fitted by the stepwise exponentials resulting from Eqs. (4a) and (4b), which leads to optimal parameters for each species: τ_0^{α}, k^{α}, and each species initial mass $m^{\alpha}(t=0) \equiv m_0^{\alpha}$. Let us mention that COMOVA code [14] is based on this approach and takes these parameters as input.

Once these parameters are known, any long term extrapolation can be performed, including the extrapolation at constant temperature displayed in Fig. 7. Because long-term extrapolation is based on the temperature acceleration modeled by Eq. (4b) or Eq. (4c), long residence times at a given temperature T_0 can only be obtained from experiments made at a higher temperature. If T_0 is already quite high, upper bounds on reachable temperatures can thus sometimes introduce practical limitations on the possible time extrapolation magnitude or on T_0.

This is an ambitious and difficult approach. It is more powerful, allowing variable temperature and taking into account reemission, and in principle is more representative of reality than the empirical approach. It is, however, not yet fully clear whether this simplified

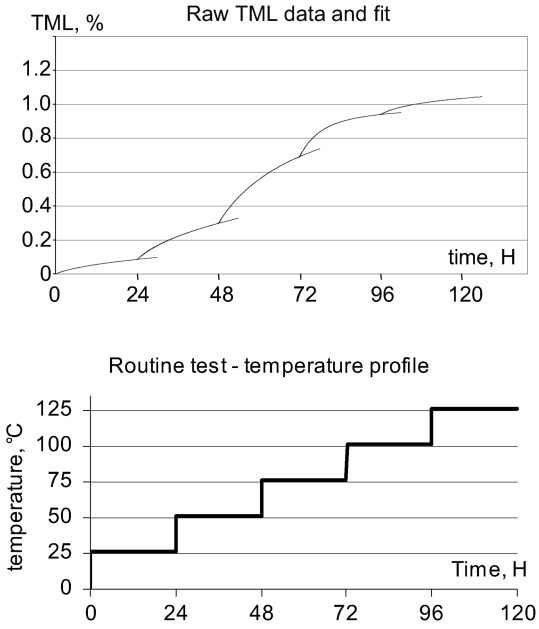

Fig. 6 Example of TML on the upper panel, with the classical stepwise temperature profile on the lower panel (ESTEC data).

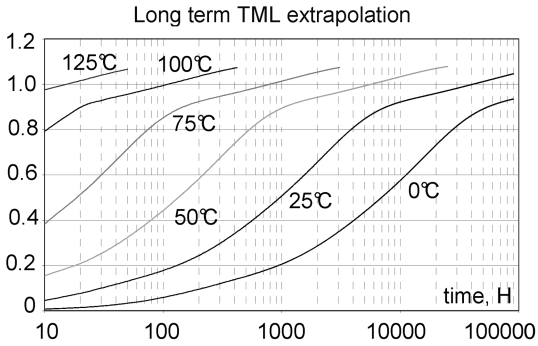

Fig. 7 Constant temperature long term extrapolation from the data above and the physical residence time approach (ESTEC data).

physical modeling is close enough to real physics to lead to better predictions. The extraction of the numerous parameters is another difficulty that impacts the global assessment process. In particular in the absence of chemical information, e.g., from mass spectrometry, the separation of species is particularly approximate. By species separations we mean attributing the total mass emitted by the sample or deposited on the QCMs to different chemical species, even chemically undetermined.

The key point in such a necessarily simplified physical approach is certainly to capture, or model, the important part of the physics and discard the superfluous part. The simplifications and assumptions of this approach are discussed in next section.

IV. Open Questions/Difficulties

A. Diffusion vs Desorption

The first open question concerning outgassing is the relative importance of diffusion and desorption in usual materials. Of course both phenomena exist and limit the outgassing rates, but for a simplified approach, determining whether outgassing is mostly diffusion limited or desorption limited is crucial.

Although the current modeling assumes a desorption-limited outgassing, while diffusion-limited outgassing is also proposed in literature [15], some elements point at a possible importance of its limitation by diffusion. For example, Fig. 8 shows toluene outgassing rate from EC2216 detected by mass spectrometry, based on mass 91 measurement by mass spectrometry. Toluene can be detected over

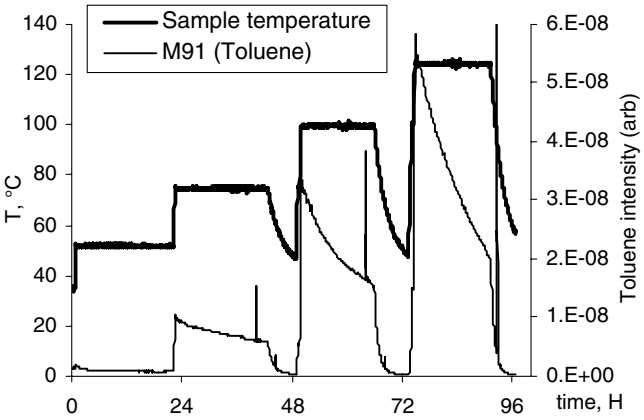

Fig. 8 Toluene emission rate from EC2216 during four temperature steps, 50, 75, 100, and 125°C (ONERA data, ESA TRP).

four successive temperature steps, from 50 to 125°C. However, modeling outgassing by desorption usually leads to species being completely emitted faster, over two or three temperature steps.

This is why it was tried to determine whether experimental data were more consistent with a limitation by diffusion or desorption. A first attempt consisted in modeling an experiment with either assumption and comparing with the data. This approach was, however, not very successful, and lead to no clear discrimination between both assumptions, probably because, on the basis of total deposit measurements, it was not possible to correctly separate species.

A second approach proved more successful. It stayed at the level of the total deposit, with no need to perform a correct species separation. The idea was to consider how outgassing rate should scale, when the diffusion length, or effective material thickness, is varied, depending on the assumption done. The studied sample was successively a reference material, typically a thin layer of glue EC2216 deposited on aluminum, and then the same layer of glue sandwiched between two foils of aluminum (Fig. 9). In the 2-D view of the figure, the diffusion length L of the sandwiched sample is no longer its width but its half

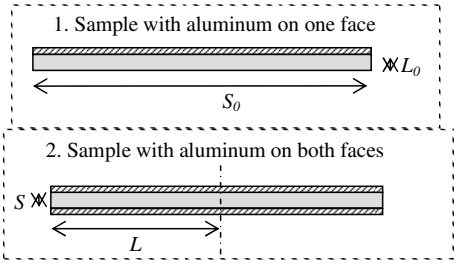

Fig. 9 Exposed surface S and effective diffusion length L of a reference sample (1) and a sandwiched sample (2).

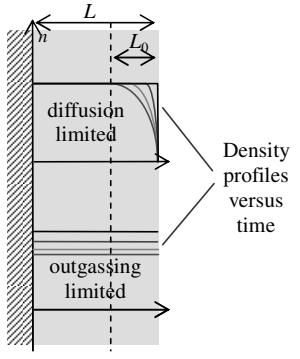

Fig. 10 Extreme cases of limitation by diffusion only (upper panel) or desorption only (lower panel).

extension. In 3-D the definition of the diffusion length was generalized as the ratio of the sample volume to its exposed surface.

It was then studied how the outgassing rate should change when going from small L_0 to large L diffusion length. In the extreme case of a pure limitation by diffusion, desorption is immediate and inefficient diffusion does not allow deep contaminants to reach the surface. In the upper panel of Fig. 10 all the successive density profiles are quasi zero at the sample surface. In the other extreme situation, diffusion is very efficient, which leads to the flat densities in the lower panel of Fig. 10, and outgassing is mostly limited, i.e., controlled, by surface desorption. In this second case the material behaves like a simple reservoir filled by contaminant, i.e., with a horizontal upper surface.

Working with the relative contaminant mass emissions ΔW defined by

$$\Delta W \equiv \frac{\Delta m_{\text{contaminant}}}{m_{\text{sample}}} \tag{5}$$

ΔW was compared with ΔW_0 for the sandwiched and reference nonsandwiched samples described in Fig. 9. In the case of the pure diffusion limitation, this is very easy. Assuming that diffusion is not effective for thickness L_0 or larger, the outgassed mass is simply proportional to the exposed sample surface S (or S_0), regardless of its effective thickness L. This assumption leads to relative masses ΔW scaling proportionally to thickness. Equation (6) presents relative contaminant mass emissions and its time derivation. Not surprisingly, both the emitted mass and its flow rate are simply reduced by the thickness ratio and follow a L_0/L scaling law

$$\Delta W(t) = \Delta W_0(t)\frac{L_0}{L} \tag{6a}$$

$$\Delta \dot{W}(t) = \Delta \dot{W}_0(t)\frac{L_0}{L} \tag{6b}$$

In the reverse situation of a limitation by desorption, the differential equation ruling outgassing, an emission flow rate proportional to the surface density, must be studied to see that the thickness change results in a time rescaling for the relative mass emission. This is not surprising because a thicker material is simply a bigger tank with the same leaking flow, as a function of the tank relative level. In this case, time derivation [Eq. (7b)] yields an extra factor. With this desorption-limited assumption, the relative mass emission ΔW is delayed, while its flow rate $\Delta \dot{W}$ is both delayed and scaled down, so that its time integral remains unchanged

$$\Delta W(t) = \Delta W_0\left(t\frac{L_0}{L}\right) \tag{7a}$$

$$\Delta \dot{W}(t) = \frac{L_0}{L}\Delta \dot{W}_0\left(t\frac{L_0}{L}\right) \tag{7b}$$

Because the scaling laws (6) and (7) are significantly different a very conclusive comparison with experimental data was expected. Next two figures (Fig. 11 and 12) display experimental mass flow rates for small and large diffusion lengths, and theoretical scaling of the reference case data to conditions of the sandwiched one, respectively ESTEC RTV S691 TML data and CNES EC2216 CVCM data. The usual five temperature-accelerated 24 H steps of Fig. 6 were transformed into an equivalent constant temperature 25°C long time series through Eq. (4c). The ESA RTV S691 was cured seven days at room temperature and spent an extra four weeks at room temperatures, while the CNES EC2216 only spent a few weeks at room temperature. For each material, the sample with large diffusion length, sandwiched between two aluminum foils, and the sample with small diffusion length, a simple layer of approximately 1 mm thickness, had the same conditioning.

The outgassing rate of the small diffusion length experiment (not sandwiched) was scaled to the large diffusion length situation

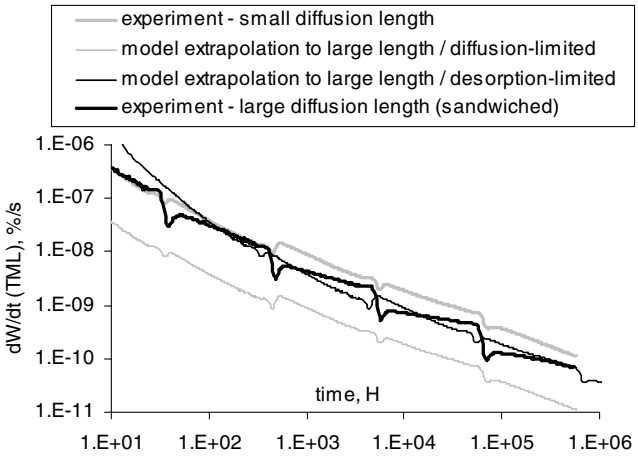

Fig. 11 Experimental TML rate (RTV S691, ESTEC data) of a reference layer, a sandwiched layer, to be compared with the former scaled according to a diffusion-limited law or a desorption-limited law.

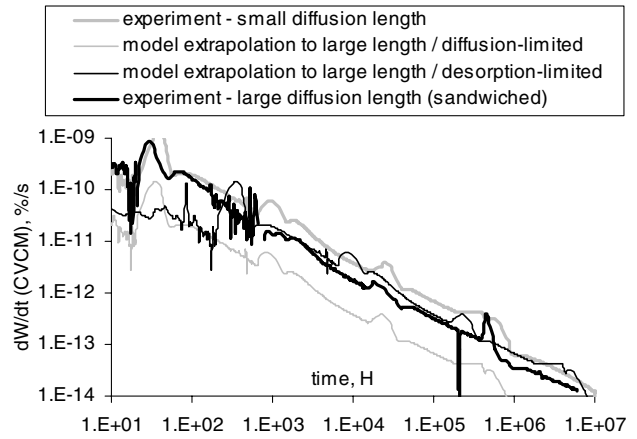

Fig. 12 Experimental CVCM deposit rate (EC2216, CNES data) of a reference layer, a sandwiched layer, to be compared with the former scaled according to a diffusion-limited law or a desorption-limited law.

(assuming a sandwiched sample) following either law above, diffusion or desorption limitation, for comparison to the other experiment.

In both cases the matching is much better, and quite good, if assuming a desorption-limited outgassing. This is a very interesting result. The conclusion is thus quite clear. In spite of the possible importance of the limitation by diffusion in some situations, as, e.g., for very large sandwiched materials, general situations look to be much more controlled by desorption.

This is a rather robust result. The reason is that an important limitation by diffusion would unavoidably lead to an L_0/L scaling of the mass flow rate. And comparison of the scaled reference data to the sandwiched data is absolutely direct, in particular not being dependent of the heating-acceleration that was applied to the time axis of the two figures above.

Other possibilities for an important role of diffusion limitation can probably only be found in special cases like very long diffusion lengths, maybe also some species that were minor in these data like very heavy ones, or maybe more likely other materials. Extra testing should also take care of a possibly different behavior above or below glass transition temperature.

B. Order 1 Law vs Order 0 Law

Another open point concerning contaminant emission is whether it should be described by an order 1 desorption law like (4) or an order 0 evaporation law such as (3). This question mostly arises for the

reemission of deposited contaminants because primary outgassing of a material is not thought to lead to thick surface layers, unless contaminant-material affinity is unlikely small.

This question may not deserve very long discussions because reasonable assumptions allow modeling simultaneously both regimes and the transition in between. Assuming a BET-like [16] structure of the deposit layers resulting from a condensation-reemission equilibrium, and neglecting the difference of affinity between molecules themselves and with the substrate the total emission rate of Eq. (8a) can be derived by summation over layers for a pure contaminant. The monolayer mass is denoted m_0. Assuming an ideal solution, i.e., the same affinity between molecules α and β as between α themselves and efficient enough mixing by diffusion, Eq. (8b) can also be derived, where m_{tot} is the total deposit mass. It can be checked that this formula asymptotically gives all the previous ones in case of submonolayer deposit (order 1 law), thick deposit (order 0 law) or a single contaminant Eq. (8a). It is also consistent with Raoult's law for ideal solutions. It will be used in our forthcoming modeling activities

$$\left(\frac{\mathrm{d}m}{\mathrm{d}t}\right)_{\text{re-emission}} = -\frac{m}{\tau_{\text{re-em}}(T)} \cdot \frac{1}{1+\frac{m}{m_0}} \tag{8a}$$

$$\left(\frac{\mathrm{d}m^{\alpha}}{\mathrm{d}t}\right)_{\text{re-emission}} = -\frac{m^{\alpha}}{\tau^{\alpha}_{\text{re-em}}(T)} \cdot \frac{1}{1+\frac{m_{\text{tot}}}{m_0}} \tag{8b}$$

C. Other Deposit Physics

However, the assumptions of ideal mixture or the absence of surface affinity are not always valid. Without considering chemical reactions that are beyond the scope of this paper, it is true that the assumptions of the last subsection are not always fulfilled. Although few answers are to be given to the questions raised, these effects were thought worth reviewing quickly here.

First the surface affinity issue, which can be generalized to both surfaces of a layer, i.e., to its vacuum interface, leads to the formation of clusters or droplets mentioned in Sec. II. This is not an uncommon experimental observation. Its consequences on the emission rates can be very large as can be seen by TGA in Fig. 13. The TGAs were performed on Bisphenol A deposits performed in presence or absence of VUV irradiation. Scanning electron microscopy (SEM) characterizations of deposits generated during a similar experiment were already reported in Fig. 2, showing that VUV irradiation led to cluster formation. The shift of a few tens of degrees in the displayed TGA are the consequence of an emission rate different by more than one order of magnitude. It was checked by gas chromatography/mass spectrometry (GC/MS) that the main TGA peak of the irradiated sample is still Bisphenol A. The main effect of UV radiation, although also leading to some photochemistry, was thus to trigger the formation of clusters.

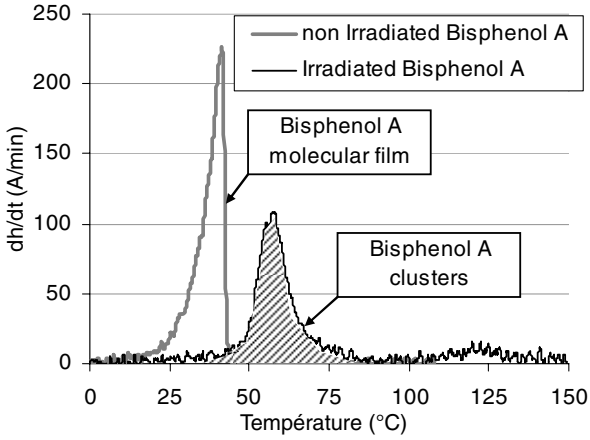

Fig. 13 Emission rates from a film or from clusters of bisphenol A during a TGA at 2°C/mn (ONERA data).

Although some modeling of droplet evaporation can be done, the formation of the droplet is too difficult to predict and practical progress in this direction does not seem easy. Their formation depends on the surface affinity, the contaminant mixture, and also seems to be quite sensitive to UV, with VUV effects having been observed in both directions depending on the situation, either favorable or unfavorable to the formation of clusters.

Similarly, nonideal mixture effects, i.e., a different affinity between homogeneous and heterogeneous molecules, are certainly too difficult to assess for any practical usage. There are too many different unknown molecules.

A different effect that leads to a violation of the ideal solution assumption is the blocking of diffusion within the deposit. The successive or simultaneous deposition of water, methanol, or toluene on a cold sample was shown [17] to have important consequences on their reemission rate, through the formation of layers. On the contrary, the presence of one monolayer of 1-alkanol seems to reduce only slightly the evaporation of water underneath [18]. It is not clear whether such situations are exceptional or could arise for typical space applications. In case of a frozen deposit another way of obtaining layer effects could be the selective evaporation or sublimation of a given compound within the top layers.

In conclusion to this section, some results of Sec. V can be mentioned in anticipation. It focuses on species separation. Within the experiment accuracy these results show the absence of mixing effects in the situation under study. Their generalization remains, however, difficult.

D. Test Procedure

In an engineering context, developing a representative physical model is not enough. Extracting the model parameters from experiments, both efficiently and accurately enough, is another requirement. A procedure must be defined in that purpose.

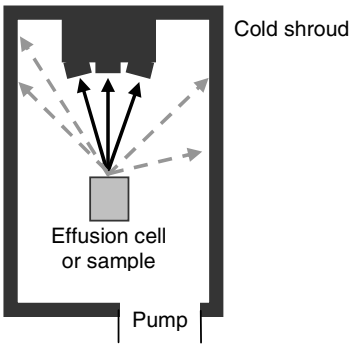

Fig. 14 Principle of a cold chamber experiment: solid trajectories contribute to QCM deposit, dashed ones do not.

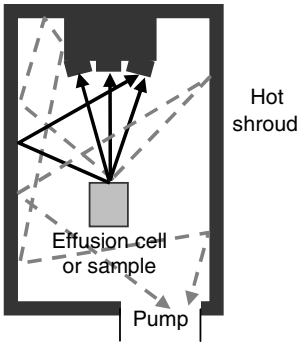

Fig. 15 Principle of a hot chamber experiment: solid trajectories contribute to QCM deposit, dashed ones do not.

A first major difficulty is species separation. Because modeling is made on a per species basis, experiments should supply a method to determine each species quantity. However the current test procedure only gives total deposits, which are difficult to split into each species contribution. This very important topic, central to this paper, is postponed to part V.

Here should only be treated another experiment-related topic, the equivalence of cold and hot chamber experiments. The simplest and most common approach is with a cold chamber or shroud. The transport is straightforward because only line-of-sight trajectories apply (see Fig. 14) and view factors can easily be computed, and of course measured.

If the chamber walls are hot, at least as hot as the effusion cell, transport is very different because reflections or reemissions happen (see Fig. 15). The fraction of contaminants that reach the QCMs is different but it can also be computed, leading to effective view factors. If the pump orifice is small enough and that no long condensation happens on the hot walls, which is in principle valid for walls warmer than effusion cell, the gas phase distributions of all species become homogeneous and isotropic. Their mass flow rates to QCMs and to the pump, the only sinks, are then proportional to the relative areas of these sinks. This leads to deposits proportional to emissions, the proportionality factors being called (effective) view factors.

A small complication arises yet when some QCMs at intermediate temperature are not a sink for all species. This effect remains negligible if the QCM areas are small compared with the pump orifice area.

E. Validation

Whatever the approach, empirical or physical, the extrapolation to flight conditions, and above all to mission duration, must be validated. The general principle consists in performing the regular test procedure and predicting another situation on this basis. For the empirical approach, the other case should be a longer test, while it can be any temperature profile in the physical approach, which claims to model any profile. Discussion will mostly focus on outgassing and condensation here, leaving aside the more difficult topic of reemission and deposit physics.

The physical approach validation was a major objective of the reported activities. Four non standard temperature profiles were defined for validation, three ramps of 12, 48, and 120 hours, and a four day long constant temperature profile visible in Fig. 16.

For reference the modeling of the TML and CVCM of a regular test with five temperature steps is plotted in Fig. 17. The outgassing model is the one described above, while CVCMs are obtained from temperature dependent sticking coefficients used in COMOVA [16]. All parameters of the model are tuned so as to obtain the best fit of the data. For each of the six species α parameters are: its initial mass m_0^α, its residence time τ_0^α, its temperature dependence coefficient k^α and two parameters describing the $S(T)$ sticking coefficient [16], because reemission matters little here.

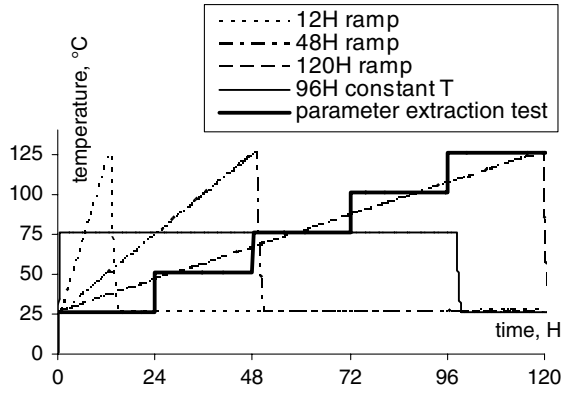

Fig. 16 Different temperature profiles for the effusion cell: the regular 5 steps routine test for reference and four validation tests.

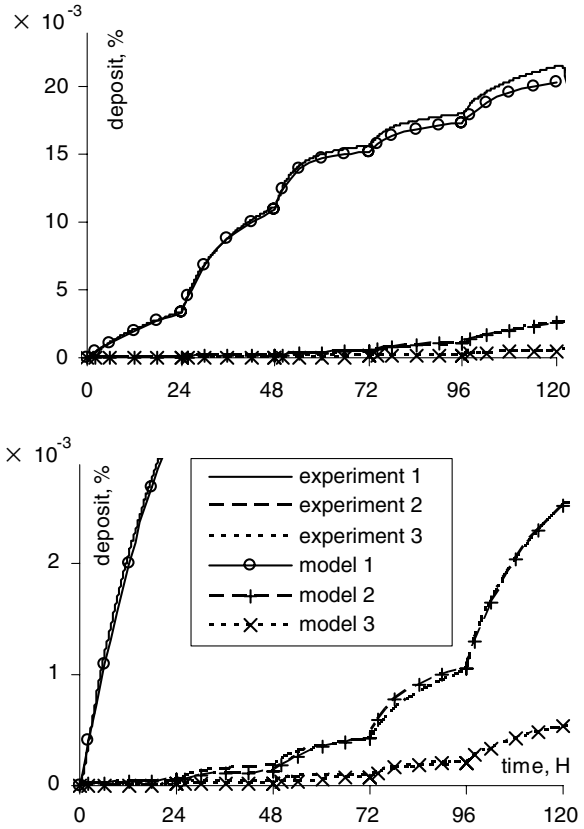

Fig. 17 Fit by the physical model of three CVCMs: experiment 1 on QCM at −150°C (hence close to a TML), experiment 2 QCM at −50°C, and experiment 3 at −10°C, five regular temperature steps of Fig. 6 for EC2216 sample. Lower panel is a close up of upper panel (CNES experiment, ONERA model, CNES R&T).

The next step was the modeling of the four validation tests with the parameters that were optimized for the regular test above. The comparison with the experimental data is given in Fig. 18. The trend is generally good, but the quantitative agreement is not very good, with a few tens of percent of discrepancy. It would be important to know how this error behaves in the longer term, but no experimental data is available. Performing such long duration tests would be needed for validation to see whether the important discrepancies of this modeling increase at larger time or not. For a constant temperature profile, the comparison with the potential discrepancies induced by a pure mathematical fit (Fig. 5) would also be interesting. The potential reasons of these discrepancies are again to be found in physical approximations, like a possible influence of diffusion-limitation on outgassing neglected here, including possible glass transitions, or in insufficient experimental data leading to a poor species separation.

V. Species Separation: Prerequisite to a Physical Modeling?

Species separation was mentioned as one of the weakest points of the physical approach as it is used today, i.e., only on the basis of global TML and CVCM measurements. If the species separation in the model is not representative of reality, the model can be viewed as a simple fit by a mathematical sum of functions, *stepwise accelerated exponentials* for first-order law (4a).

Two main improvements of the tests were considered. Because global deposits do not supply any direct information on the species, other measurement techniques had to be considered. The first idea consists in performing TGAs of the deposit. Such TGA results are presented in [19]. Although limited to a global mass measurement, progressive heating of a QCM results in some species separation. The separation, made on physical grounds, will not distinguish different

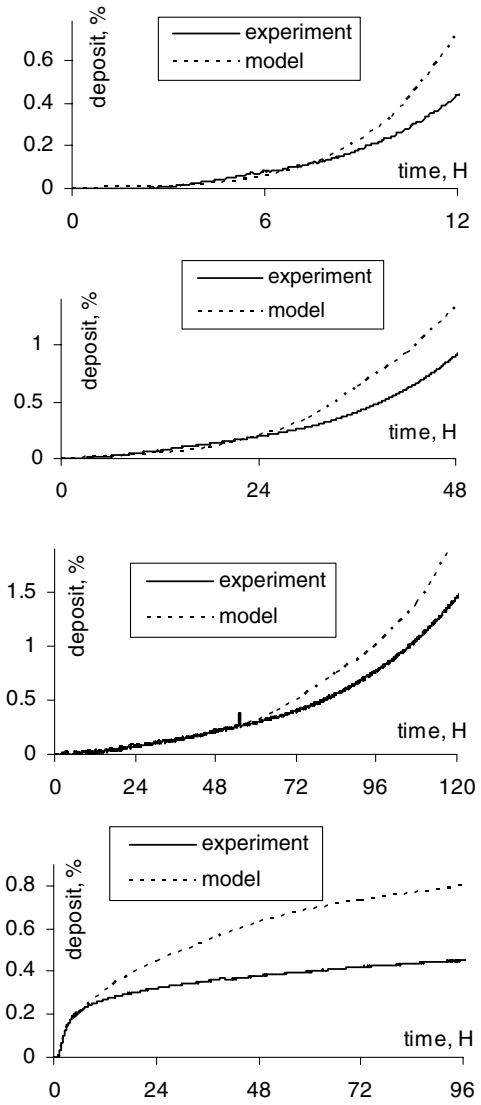

Fig. 18 The four validation TML tests (temperature profiles of Fig. 16): experiment and model with parameters determined from the standard test (CNES experiment, ONERA model, CNES R&T).

chemical species of similar physical properties such as residence time. It might yet be sufficient for engineering purposes [19].

The second possible improvement is the usage of a mass spectrometer or residual gas analyzer (RGA), necessarily in conjunction with some separation technique because otherwise mass spectra of too many species combine and make interpretation impossible. Less accurate than gas chromatography, but much easier to implement, in particular in situ, thermogravimetric analysis was used to perform some species separation. It might not become part of the routine test procedure to be defined, but proves at least very useful at research level.

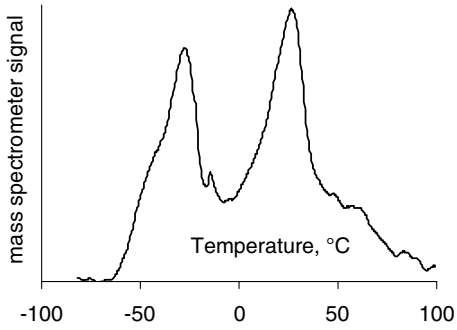

Fig. 19 Example of TGA (2 K/mn) of a contaminant deposit originating from EC2216 (ONERA data).

As a first example, Fig. 19 displays the mass flow rate evaporating from a QCM during a TGA (2°C/mn) after contamination at −75°C by EC2216 outgassed at 125°C. The presence of distinct peaks indicates that this method should allow performing some species separation. But the fact that they are overlapping shows that this separation cannot perfect based on this simple TGA information.

Using also an RGA allows a better interpretation [20]. Six masses are displayed on Fig. 20. Masses 109 and 125 seem representative of two different chemical species, showing that the second peak is probably due to at least two species. Its slow decrease is also probably due to several species, as can be deduced from masses 36 and 212. The first peak is also at least double, as visible on masses 47 and 94, both contributing but with different shapes. It is thus clear that MS measurements are an important improvement to TGA. The extra effort needed is, however, also important. It is thus not clear today whether mass spectrometry should be part of new routine tests in the future.

TGAs from deposits collected on QCMs at different temperatures, from similar fluxes, were also performed. Grouping in the same graph the TGAs from QCMs that were maintained at 0, −25, −50, and −75° during the deposition phase, very interesting features appear (Fig. 21).

First, TGAs are very similar at high temperatures: low volatility species were condensed similarly and are reemitted similarly. There is no important mixing effect due to different content in volatile species.

Second, the zone where two TGAs differ is always approximately 40°C after the TGA on the warmest QCM starts. In the same zone it can also be noticed that the first 30°C of each TGA gives no emission at all, up to experimental uncertainty. The explanation is quite

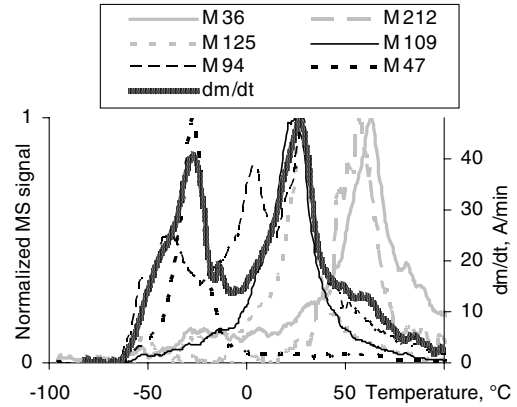

Fig. 20 The same TGA with six concomitant mass measurements by mass spectrometry (ONERA data).

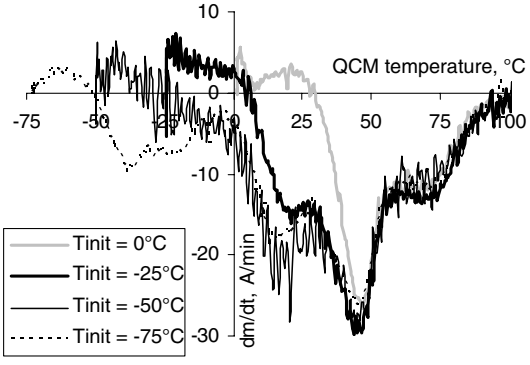

Fig. 21 TGAs performed on four QCMs (at 2 K/mn) which were initially submitted to the same contaminant flux from ECC2216 while being maintained at four different temperatures (ESA TRP, ONERA data).

straightforward. A QCM that spent 24 hours at, e.g., 0°C was subject to some evaporation. At the TGA start, the crystal remains a few minutes in the (0–30°C) range. Hence evaporation is only possible for molecules of which residence time at 30°C is less than a few minutes. However, they previously spent 24 H at 0°C and can only be present at TGA start if their residence time at 0°C was longer than 24 H. Therefore, this *blind zone* of 30 or 40°C at the start of the TGAs is explained by reemission before the TGA, and it can be checked that its size is consistent with typical activation energies because a 24 H residence time becomes on the order of the minute for a temperature increase close to 30–40°C.

This clearly explains the observed difference between the TGAs at the beginning of the TGA on the warmest QCM. Therefore, if the first 40°C of a TGA are excluded, it can be concluded for this example that a TGA from a warmer QCM does not provide more information than a TGA from a colder QCM because it can simply be deduced from the latter. If this result is confirmed on other materials, it will have important practical consequences. Only one cold QCM may be needed and its TGA should allow determining what would be the deposit at another temperature.

The theoretical aspects of this result are also interesting. Although this is certainly not true at detail level, this shows that on this case mixing effects are not very important. For example the presence of the species evaporated around -40 on the $-75°$ QCM were not present on the $-50°$ QCM. However, the evaporation of other species around $+10 - 20$°C is unaffected. Of course such mixing effects are more likely to show up for species with closer evaporation temperatures.

VI. Conclusions

The physical grounds of contamination and of the two major approaches to its practical assessment, either empirical or physical, were reviewed. The questions still open to improve and validate the ambitious physical approach were discussed. Original results stemming from important recent efforts in ESA, CNES, and ONERA to validate this approach were presented next.

The first important conclusion is the predominance of the limitation by desorption over the limitation by diffusion in the outgassing process. This was quite clear both for the mass loss experiments and the condensation experiments conducted at ESTEC and CNES, respectively. In both cases the theoretical scaling of the experimental data involving a small diffusion length to another situation involving a large diffusion length matched the experimental data of the long diffusion length situation (sandwiched sample) if a dominantly desorption-limited outgassing was assumed, whereas it did not if a diffusion-limited outgassing was assumed. The generalization of this result beyond the RTV S691 and EC2216 samples under study was not performed. Doing so empirically by extensive testing is costly, while doing so on theoretical grounds is difficult, but may be an interesting idea.

The second important result was an attempt to validate the physical approach as it is used today, i.e., without an accurate species separation. The parameters of the physical model were extracted from the routine test and used to model different temperature profiles, three different ramps and a four-day-long isothermal test. The comparison to experimental data exhibited a reasonable agreement, typically within a factor 1.5.

The last important result was the rather linear behavior of deposits in thermogravimetric analyses. The TGAs performed on QCMs at different temperatures were very similar in most of the common temperature interval of the TGA. It proved that, although they were observed in special situations elsewhere, morphology effects, surface affinity effects or species mixing effects were negligible in this case. Generalization of this result, although very desirable, remains difficult again.

Acknowledgments

The results obtained at ONERA were funded by Centre National d'Etudes Spatiales Research and Technology and ESA Technology Research Programme, for which ONERA authors are very grateful to CNES and ESA. These results were obtained in close collaboration between Centre National d'Etudes Spatiales, ESA, and ONERA. They involved activities in all companies.

References

[1] Van Eesbeek, M., and Zwaal, A., "Outgassing and Contamination Model Based on Residence Time," *Proceedings of the 3rd European Symposium on Spacecraft Materials in Space Environment*, European Space Research and Technology Centre , Noordwijk, The Netherlands, 1985, pp. 25–34.

[2] Nghiem, M.-P., Tondu, T., Roussel, J.-F., and Faye, D., "Molecular Thin Film Chemical Modifications Under Vacuum Ultraviolet Irradiation," *Journal of Vacuum Science and Technology A (Vacuum, Surfaces, and Films)*, Vol. 28, No. 1, Jan–Feb 2010, pp. 119–126.

[3] Pereira, A., Roussel, J.-F., Van Eesbeek, M., Schmeitzsky, O., and Faye, D., "Experiments and Physical Modeling of Ultraviolet-Enhanced Contamination from Pure Contaminants," *Journal of Spacecraft and Rockets*, Vol. 43, No. 2, 2006, pp. 402–409. doi:10.2514/1.14955

[4] Jenkins, R. M., Ciucci, A., and Cochran, J. E. Jr., "Simplified Model for Calculation of Backflow Contamination from Rocket Exhausts in Vacuum," *Journal of Spacecraft and Rockets*, Vol. 31, No. 2, March–April 1994, pp. 265–270.

[5] Nadiradze, A. B., Obukhov, V. A., and Popov, G. A. "Electric Propulsion Plasma Plume Interaction with "Phobos-Soil" Spacecraft Structural Components," *Acta Astronautica* Vol. 64, Nos. 9–10, 2009, pp. 979–987. doi:10.1016/j.actaastro.2008.12.018

[6] Masaro, L.358, and Zhu, X. X., "Physical Models of Diffusion for Polymer Solutions, Gels and Solids," *Progress in Polymer Science*, Vol. 24, No. 5, 1999, pp. 731–775. doi:10.1016/S0079-6700(99)00016-7

[7] Wang, B.-G., Lv, H-L., and Yang, J.-C, "Estimation of Solvent Diffusion Coefficient in Amorphous Polymers Using the Sanchez–Lacombe Equation of State," *Chemical Engineering Science*, Vol. 62, No. 3, 2007, pp. 775–782. doi:10.1016/j.ces.2006.10.020

[8] Chu, L.-Q., Mao, H.-Q., and Knoll, W., "In Situ Characterization of Moisture Sorption/Desorption in Thin Polymer Films Using Optical Waveguide Spectroscopy," *Polymer*, Vol. 47, No. 21, 2006, pp. 7406–7413. doi:10.1016/j.polymer.2006.08.031

[9] Fong M. C, "Surface Adsorption-Migration Kinetics," *Journal of Vacuum Science and Technology A (Vacuum, Surfaces, and Films)*, Vol. 9, No. 2, March–April 1991, pp. 207–211. doi:10.1116/1.577522

[10] Stewart, T. B., Arnold, G. S., Hall, D. F., Marvin, D. C., Hwang, W. C., Young Owl, R. C., and Marten, H. D., "Photochemical Spacecraft Self-Contamination: Laboratory Results and Systems Impacts," *Journal of Spacecraft and Rockets*, Vol. 26, No. 5, Sept.–Oct. 1989, pp. 358–367.

[11] Roussel J.-F., Alet, I., Faye, D., and Pereira, A., "The Effect of Space Environment on Spacecraft Surfaces on Sun-Synchronous Orbits," *Journal of Spacecraft and Rockets*, Vol. 41, No. 5, 2004, pp. 812–820. doi:10.2514/1.1211

[12] ASTM E 1559, "Standard Test Method for Contamination Outgassing Characteristics of Spacecraft Materials," American Society for Testing and Materials Committee E-21, 1993.

[13] Roussel, J.-F., Lemcke, C., Giunta, I., Van Eesbeek, M., and Sorensen, J., "Contamination Modeling: Underlying Principles and First Examples for a New Software," *Proceedings of the 8th International Symposium on Materials in a Space Environment*, CNES, Arcachon, France, 2000.

[14] Arnold, G. S., "Spacecraft Contamination Model Development," *Proceedings of SPIE: The International Society for Optical Engineering*, Vol. 3427, 1998, pp. 272–289.

[15] Fang, W., Shillor, M., Stahel, E., Epstein, E., Ly, C., McNiel, J., and Zaron, E., "A Mathematical Model for Outgassing and Contamination," *Journal of Applied Mathematics*, Vol. 51, No. 5, 1991, pp. 1327–1355.

[16] Brunauer, S., Emmet, P. H., and Teller, E., "Adsorption of Gases in Multimolecular Layers," *Journal of the American Chemical Society*, Vol. 60, No. 2, 1938, pp. 309–319. doi:10.1021/ja01269a023

[17] Phillips, T. E., Bargeron, C. B., and Benson, R. C., "Thermogravimetric Analysis of Selected Condensed Materials on Quartz Crystal Microbalance," *Journal of Vacuum Sciences and Technology A:*

Vacuum, Surfaces, and Films, Vol. 13, No. 6, Nov. 1995, pp. 2726–2731.

[18] Rusdi, M., and Moroi, Y., "Study on Water Evaporation Through 1-Alkanol Monolayers by the Thermogravimetry Method," *Journal of Colloid and Interface Science*, Vol. 272, No. 2, 2004, pp. 472–479. doi:10.1016/j.jcis.2004.01.014

[19] Simpson, T. R., Hall, D. F., and Ternet, G. K., "Extraction of Properties of Condensed Outgassed Species by Thermogravimetric Analysis," *Proceedings of SPIE: The International Society for Optical Engineering*, Vol. 4774, 2002, pp. 150–159.

[20] Raemaekers, K. G. H., and Bart, J. C. J., "Applications of Simultaneous Thermogravimetry-Mass Spectrometry in Polymer Analysis," *Thermochimica Acta*, Vol. 295, 1997, pp. 1–58. doi:10.1016/S0040-6031(97)00097-X

D. Edwards
Associate Editor